Monthly Notices
of the
ROYAL ASTRONOMICAL SOCIETY

Mon. Not. R. Astron. Soc. **401,** 1369–1374 (2010) doi:10.1111/j.1365-2966.2009.15737.x

Predicting gamma-ray burster redshifts from their prompt emission properties

Chris Koen★

Department of Statistics, University of the Western Cape, Private Bag X17, Bellville, 7535 Cape, South Africa

Accepted 2009 September 18. Received 2009 September 13; in original form 2009 March 26

ABSTRACT

This paper presents a study of the relation between gamma-ray burster redshift and several of its prompt emission properties (spectral lag, light curve variability, peak energy, rise time and the peak bolometric flux $P_{\rm bol}$). Simple predictors of $\log(1+z)$ in terms of $P_{\rm bol}$ and the other indicators are derived. The typical scatter in the relations is 0.13 dex. An illustrative application to observations of GRB 090423 ($z \sim 8$) is given.

Key words: methods: statistical – gamma-rays: bursts.

1 INTRODUCTION

There is a fairly large body of published work on gamma-ray burster (GRB) luminosity indicators (see Koen 2009 for some of the many references). By contrast, there have been surprisingly few papers on the related, but none the less distinct, problem of the prediction of GRB redshifts from prompt gamma-ray observables. Atteia (2003) calculated the theoretical dependence on redshift z of the quantity

$$X = \frac{N_\gamma T_{0.90}^{0.5}}{E_{\rm p}}, \tag{1}$$

where N_γ is the number of emitted photons, $T_{0.90}$ the time interval during which the central 90 per cent of the GRB flux was detected and $E_{\rm p}$ the GRB energy spectrum peak. The dependence is described by a function which is slightly non-linear in a log–log plot of X against redshift. There is one free parameter (the intercept of the log–log graph), which is determined from 17 GRBs for which all the required parameters have been measured. The inverse of the calibrated log X–log z function can then be used to estimate redshifts.

Pélangeon et al. (2006) replaced X in (1) by

$$X' = \frac{N_{15}}{E_{\rm p}}\ , \tag{2}$$

where N_{15} is the total photon flux over the 15 s interval of maximum fluence. The theoretical relation between X' and z is calibrated using measurements for 19 GRBs.

A similar approach was used by Firmani et al. (2006) to establish a statistical relationship between redshift and the quantity

$$X'' = \frac{P_{\rm bol} T_{0.45}^{0.49}}{(1+z)^{0.2} E_{\rm p}^{1.62}}\ , \tag{3}$$

where $P_{\rm bol}$ is the bolometric peak flux, and $T_{0.45}$ is defined similarly to $T_{0.90}$ above (with 45 per cent replacing 90 per cent). Data for 19 GRB were used in the calibration.

Zhang et al. (2006) introduced the 'relative spectral lag (RSL)', i.e. the time lag between GRB variations measured in two different energy channels, standardized by a measure of the pulse width observed in one of the channels. As the brief description implies, the RSL is defined for GRB in which a single burst pulse is seen. The authors find a linear relation between redshift and RSL for nine GRBs. Unfortunately, only one of the nine redshifts was determined from a spectrum – the remaining eight were estimated from a relation (Yonetoku et al. 2004) between $E_{\rm p}$ and the GRB peak luminosity. Formally, this means that Zhang et al. (2006) have established a possible statistical relationship between RSL, $E_{\rm p}$ and peak luminosity – a connection to redshift still needs to be demonstrated using directly measured redshifts.

Schaefer (2007) combined several luminosity indicators to produce estimates of GRB distance moduli and then derived redshifts from the latter.

In this paper, a more systematic, data-driven approach is taken. Use is made of the extensive data compilation of Schaefer (2007), who tabulated a range of light curve and spectral properties of 69 GRBs for which directly measured redshifts are available. Below, redshifts are regressed on bolometric peak $P_{\rm bol}$ and various combinations of the spectral lag $\tau_{\rm L}$ between hard and soft radiation, the GRB peak energy $E_{\rm p}$, the minimum light curve rise time $\tau_{\rm R}$ and a measure V of the 'spikiness', or level of intrinsic variability, of the GRB lightcurve (see Schaefer 2007 for details). The regression model is formulated in Section 2, and two important simplifications in the approach are discussed. A table of satisfactory models (i.e. models for which all coefficients are significant) is presented, and discussed, in Section 3. In Section 4, the results are briefly compared with those from the papers mentioned above. Section 5 applies the models to observation of a recently discovered GRB thought to have a very high redshift. A few concluding remarks are given in Section 6.

★E-mail: ckoen@uwc.ac.za

2 PRELIMINARIES

The basic relation to be studied is

$$\log(1+z) = \beta_0 + \beta_1 \log P_{\rm bol} + \sum_{j=1}^{K} \beta_{j+1} \log x_j + \text{error}, \qquad (4)$$

where x_j are independent variables (selected from the list $\tau_{\rm L}$, V, $E_{\rm p}$ and $\tau_{\rm R}$) and the β_i ($i = 1, 2, \ldots, K$) are regression constants. Before proceeding, two points are worth discussing. The first is the influence of measurement errors in $P_{\rm bol}$ and x_j. The second is the fact that $P_{\rm bol}$ is an explicit function of the dependent variable, the redshift.

A potential complicating factor in the estimation of the β_i is the substantial measurement errors in the independent variables. Strictly speaking, in order to formally accommodate the measurement uncertainties, so-called 'errors-in-variables' regression should be performed (e.g. Fuller 1987). This was investigated for GRB luminosity indicators by Koen (2009), also using the Schaefer (2007) data. His results showed that the model coefficients obtained from ordinary least squares (OLS) differed by less than one standard error from those estimated by weighted errors-in-variables regression. Since the errors-in-variables procedures are rather more involved, the simple expedient of OLS estimation will be followed in this paper. It is noted though that as more data become available, standard errors of estimated parameters will decrease and errors-in-variables regression will be worthwhile.

We now turn to the problem posed by the explicit dependence of $P_{\rm bol}$ on redshift. It is demonstrated that, fortunately, the dependence is weak and it can be neglected in a first approximation. Expressions for the bolometric peak flux $P_{\rm bol}$ are taken from Schaefer (2007), and repeated here, as these are important in what follows:

$$P_{\rm bol} = P \begin{cases} I_2/I_1, & \text{if P in energy flux units} \\ I_2/I_0, & \text{if P in photon flux units,} \end{cases} \qquad (5)$$

where P is the observed peak flux. The I_i ($i = 0, 1, 2$) in (5) are

$$I_0 = \int_{E_{\rm min}}^{E_{\rm max}} \Phi(E)\,{\rm d}E$$

$$I_1 = \int_{E_{\rm min}}^{E_{\rm max}} E\,\Phi(E)\,{\rm d}E$$

$$I_2 = \int_{1/(1+z)}^{10\,000/(1+z)} E\,\Phi(E)\,{\rm d}E, \qquad (6)$$

where $E_{\rm min} \le E \le E_{\rm max}$ is the energy range covered by the detector and $\Phi(E)$ is the observed GRB energy spectrum. The latter is assumed to be of the form

$$\Phi(E) = A \begin{cases} E^{\alpha} {\rm e}^{-qE}, & E \le E_* \\ E_*^{\alpha-\beta} {\rm e}^{-qE_*} E^{\beta}, & E > E_* \end{cases}, \qquad (7)$$

where A is a scaling constant, and

$$q = \frac{2+\alpha}{E_{\rm p}} \qquad E_* = \frac{\alpha-\beta}{2+\alpha} E_{\rm p}\,,$$

and α and β are constants.

After some algebra

$$I_1 = A \left[\frac{E_*^{\alpha-\beta}}{\beta+2} {\rm e}^{-qE_*} \left(E_{\rm max}^{\beta+2} - E_*^{\beta+2} \right) + \frac{1}{q^{\alpha+2}} \int_{qE_{\rm min}}^{qE_*} {\rm e}^{-y} y^{1+\alpha}\,{\rm d}y \right]$$

$$I_0 = A \left[\frac{E_*^{\alpha-\beta}}{\beta+1} {\rm e}^{-qE_*} \left(E_{\rm max}^{\beta+1} - E_*^{\beta+1} \right) + \frac{1}{q^{\alpha+1}} \int_{qE_{\rm min}}^{qE_*} {\rm e}^{-y} y^{\alpha}\,{\rm d}y \right] \qquad (8)$$

is obtained. The result for I_2 is similar to that for I_1: $E_{\rm max}$ and $E_{\rm min}$ are just replaced by $10\,000/(1+z)$ and $1/(1+z)$, respectively. The integrals in the expressions for I_1 and I_2 can be written in terms of upper incomplete gamma functions

$$\gamma(a, x) \equiv \int_0^x {\rm e}^{-y} y^{a-1}\,{\rm d}y \qquad a > 0 \qquad (9)$$

giving

$$I_1 = A \left[\frac{E_*^{\alpha-\beta}}{\beta+2} {\rm e}^{-qE_*} \left(E_{\rm max}^{\beta+2} - E_*^{\beta+2} \right) + \frac{1}{q^{\alpha+2}} \gamma(\alpha+2, qE_*) - \gamma(\alpha+2, qE_{\rm min}) \right]$$

$$I_2 = A \left\{ \frac{E_*^{\alpha-\beta}}{\beta+2} {\rm e}^{-qE_*} \left[\left(\frac{10000}{z} \right)^{\beta+2} - E_*^{\beta+2} \right] + \frac{1}{q^{\alpha+2}} \left[\gamma(\alpha+2, qE_*) - \gamma\left(\alpha+2, \frac{q}{z}\right) \right] \right\} \qquad (10)$$

The integral in the expression for I_0 cannot be written in terms of gamma functions because the requirement $a > 0$ in (9) implies that $\alpha > -1$ should hold – which is not the case for most of the GRBs in table 2 of Schaefer (2007).

The standardizing functions I_0 and I_1 do not depend on the redshift; $P_{\rm bol}$ in (2) is a function of redshift only through I_2, and the redshift dependence is made explicit in (10). The contribution of the last term in (10), as a fraction of the whole, is plotted in Fig. 1. For the low-energy GRB 020903 ($E_{\rm p} = 2.6$ keV) the figure is about 0.27; for GRB 990712 ($\alpha = -1.88$) the figure is 0.11. For the remainder of the GRB the last term is essentially negligible. This means that for practical purposes the redshift dependence of $P_{\rm bol}$ is of the form

$$P_{\rm bol} = c_1 + c_2 z^{-\beta-2},$$

where c_1 and c_2 do not depend on z. Since generally β is close to -2 (the average being -2.2), the explicit dependence of $P_{\rm bol}$ on redshift is quite weak and can be neglected to a first approximation.

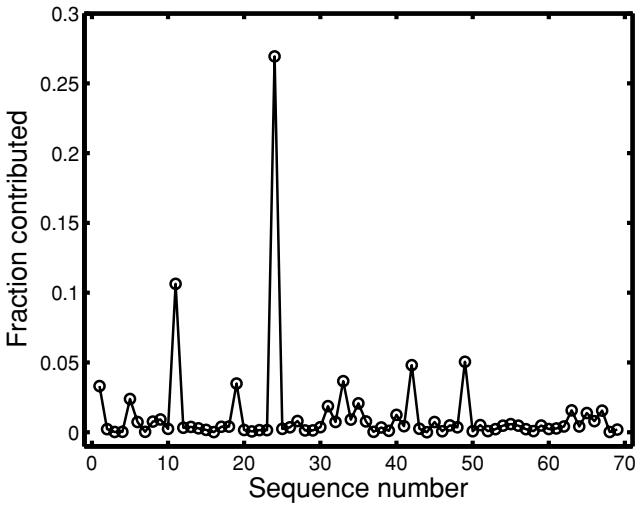

Figure 1. The fractional contribution of the last term in (10) to the full value. The horizontal axis shows the sequence number of the GRB in table 2 of Schaefer (2007).

3 RESULTS

All 15 subsets of $\tau_{\rm L}$, V, $E_{\rm p}$ and $\tau_{\rm R}$, as well as the model which uses none of these, were estimated. All the models in which all the

Table 1. The results of fitting the OLS model specified in equation (4) to the data in table 4 of Schaefer (2007).

Model	Intercept	$P_{\rm bol}$	$\tau_{\rm L}$	V	$E_{\rm p}$	$\tau_{\rm R}$	σ_e	σ_z	N
1	−0.30 (0.16)	−0.12 (0.03)					0.17	1.31	69
2	−1.09 (0.22)	−0.24 (0.03)	−0.19 (0.04)				0.11	0.90	38
3	−0.34 (0.17)	−0.19 (0.03)		0.14 (0.07)			0.14	1.18	51
4	−1.59 (0.25)	−0.24 (0.03)			0.30 (0.05)		0.13	1.10	64
5	−0.80 (0.17)	−0.20 (0.03)				−0.15 (0.04)	0.14	1.20	62
6	−1.83 (0.30)	−0.29 (0.03)	−0.18 (0.03)		0.20 (0.06)		0.10	0.85	36
7	−1.23 (0.33)	−0.26 (0.04)		0.14 (0.07)	0.23 (0.07)		0.13	1.12	48
8	−1.81 (0.26)	−0.28 (0.03)			0.26 (0.05)	−0.14 (0.04)	0.12	1.04	57

Note. Estimated standard errors are given in brackets. The residual standard deviation is denoted by σ_e, and N is the number of GRB included in the regression. The predicted values of the actual redshift z [rather than $\log(1+z)$] were also compared to the observed values: the scatter is given in the column headed σ_z.

estimated parameters were significant (i.e. coefficients at least two standard errors in size) are listed in Table 1.

In order to use these relations in practice to estimate a redshift, the following are suggested

(i) If more than one independent variable is available, select one of the multiple-indicator relations from Table 1.
(ii) Assume a preliminary redshift $z_0 = 1$ and calculate $P_{\rm bol}$.
(iii) Estimate the redshift, using the relation selected in (i).
(iv) Recalculate $P_{\rm bol}$, using the redshift from (iii).
(v) Iterate a few times over (iii) and (iv).

The performance of the regression relations is now illustrated using the data from Schaefer (2007) (tables 2 and 4). The procedure is to compare predicted redshifts to observed values. Data for one GRB are excluded and the regression relation re-estimated (so that it does not depend on the data for the deselected GRB). The newly estimated regression equation is then used to estimate the redshift of the deselected GRB, using the recipe above. The procedure is repeated N times, deselecting each of the N GRB in turn. Some of the results are shown in Figs 2–4: it is clear that the iteration over redshift [steps (iii)–(v) in the recipe above] makes little difference, as may have been anticipated from the discussion in Section 2. The scatter in the predicted versus observed diagrams is consistently 0.01 larger than the σ_e given in Table 1. Table 1 also shows the scatter when comparing observed and predicted redshifts [as opposed to values of $\log(1+z)$]; these results are denoted by σ_z.

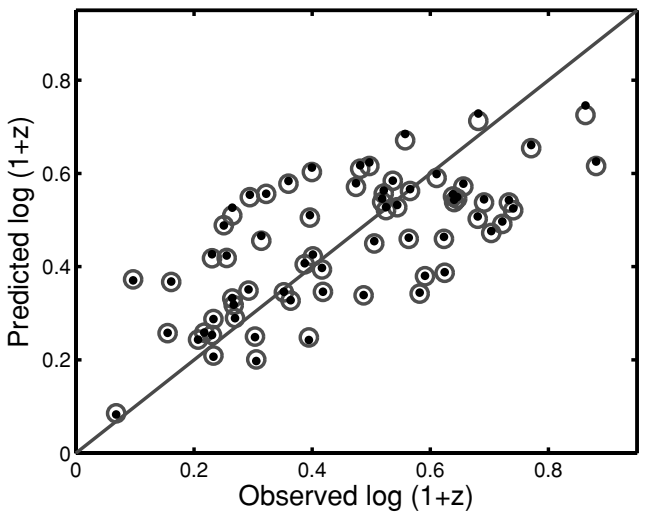

Figure 2. Observed redshifts compared to predictions generated as described at the end of Section 3. Circles are the predicted values from Model 4 in Table 1 (i.e. based on $P_{\rm bol}$ and $E_{\rm p}$ as independent variables); dots are corrected values, obtained by iterating over redshift (see the recipe in Section 3). The diagonal line denotes equality of the two variables.

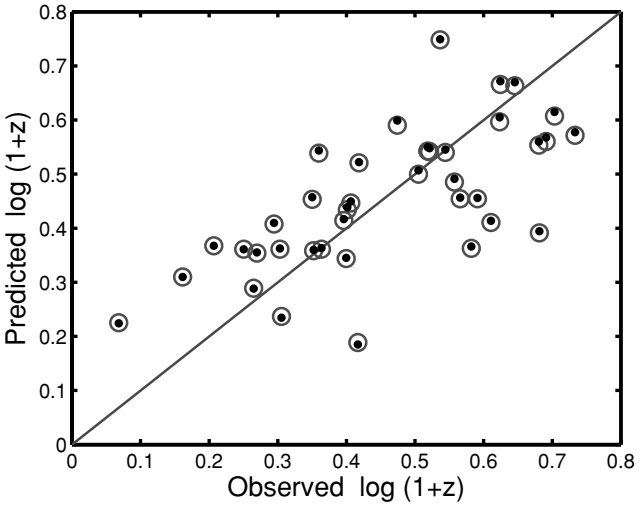

Figure 3. As for Fig. 2, but based on Model 2 (i.e. using $P_{\rm bol}$ and $\tau_{\rm L}$ as independent variables).

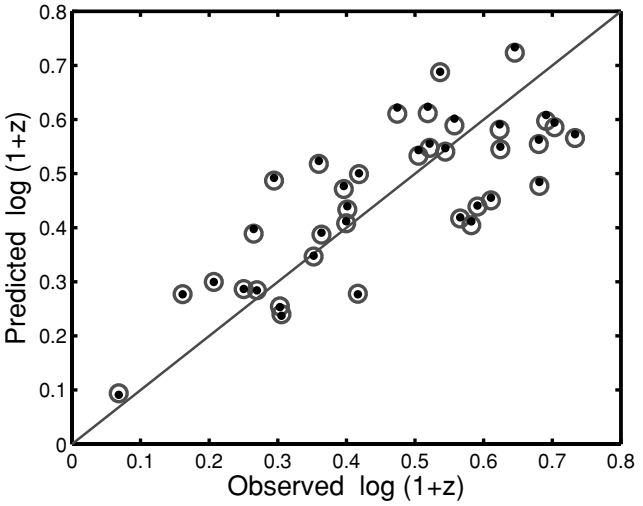

Figure 4. As for Fig. 2, but based on Model 6 (i.e. using $P_{\rm bol}$, $\tau_{\rm L}$ and $E_{\rm p}$ as independent variables).

4 COMPARISON WITH PREVIOUS RESULTS

It is interesting to compare the scatter in predicted redshifts [as opposed to comparing values of $\log(1+z)$] of models in Table 1 with those obtained from calibrations in the literature. To that end, the focus in this section is primarily on Models 2, 4 and 6.

Atteia (2003) obtained a scatter of $\sigma_z = 0.90$ over his 17 predicted redshifts. The three regression models mentioned above were applied to GRB which are in both the Schaefer (2007) and Atteia (2003) samples. Values of σ_z comparable to those of Atteia (2003) were obtained. Prediction of the redshift of GRB 000131 is poor using Atteia's (2003) relation (observed value 4.5, predicted value 1.35). The redshift of this object can be estimated using all variables in Table 1 except $\tau_{\rm L}$ (which is not given in Schaefer 2007): for single variables (in addition to $P_{\rm bol}$), predictions are 1.99–2.58 (Models 3–5); for Models 7 and 8, $\widehat{z} = 2.24$ and 3.03 are, respectively, obtained. The relatively poor performance of the Atteia (2003) predictor for this high-redshift GRB is perhaps not surprising, as only three of his/her 17 calibrating GRBs had redshifts in excess of 2.

The scatter in $z - \widehat{z}$ (24 values) for the Pélangeon et al. (2006) relation is $\sigma_z = 0.47$. Comparable scatter is obtained for Models 2 and 4 ($\sigma_z = 0.50$ and 0.46, respectively), when these are used to predict the redshifts of the 16 GRBs for which $\tau_{\rm L}$ are available. The scatter obtained from Model 4 predictions, for data overlapping with those of Pélangeon et al. (2006), is somewhat larger – $\sigma_z = 0.76$, for 22 GRBs.

The Pélangeon et al. (2006) sample of of 24 GRBs contained only two with redshifts in excess of 3 ($z = 3.2$, 3.37).

The differences between observed and predicted redshifts in table 4 of Firmani et al. (2006) are also small – $\sigma_z = 0.51$ (sample size 20, three redshifts higher than $z = 2$). For those GRBs also in the Schaefer (2007) sample, and with $\tau_{\rm L}$ measured ($N = 13$), the Firmani et al. (2006) scatter is $\sigma_z = 0.60$, whereas redshifts predicted from Models 2 and 6 have $\sigma_z = 0.48$ and 0.47, respectively. For Model 4, $\sigma_z = 0.78$, compared to $\sigma_z = 0.51$ for the Firmani et al. (2006) relation ($N = 19$). The largest discrepancy between observed and predicted redshift for the Firmani et al. (2006) sample is for GRB 020124 ($z = 3.198, \widehat{z} = 1.797$). By comparison, the Table 1 relations give $1.86 \leq \widehat{z} \leq 2.93$ (Models 2–5) and $2.27 \leq \widehat{z} \leq 2.79$ (Models 6–8).

Comparison with the estimated redshifts of Schaefer (2007) is facilitated by first noting that the luminosity distance is

$$d_{\rm L} = \frac{c}{H_0}(1+z)\int_0^z \frac{{\rm d}u}{\sqrt{(1+u)^3\Omega_{\rm M}+\Omega_\Lambda}} \equiv \frac{c}{H_0} f(z). \qquad (11)$$

For $\Omega_\Lambda = 1 - \Omega_{\rm M}$ and $\Omega_{\rm M} = 0.27$, the approximation

$$\log f(z) \approx 0.20 + 1.20 \log z \qquad (12)$$

is quite accurate over the range $0.1 \leq z \leq 10$ (the maximum difference between the left- and right-hand sides is 0.03). Schaefer (2007), table 6, contains estimates of GRB distance moduli

$$\mu = 5 \log d_{\rm L} - 5.$$

It follows from (11) and (12) that

$$\log z \approx -0.833 \log\left(\frac{c}{H_0}\right) + \frac{1}{6}\mu + 0.667 = -7.345 + \frac{1}{6}\mu \qquad (13)$$

($H_0 = 75\ {\rm km\,s^{-1}\,Mpc^{-1}}$).

A plot of predicted redshift against observed redshift can be seen in fig. 9 of Schaefer (2007); the agreement between two quantities is quite good. The scatter is

$$\sigma_e' = \left[\frac{1}{N}\sum_j (\log z - \log\widehat{z})^2\right]^{1/2} = 0.11$$

$$\sigma_z = \left[\frac{1}{N}\sum_j (z - \widehat{z})^2\right]^{1/2} = 0.60$$

which can be compared to σ_e and σ_z in Table 1.

It should be said though that the *observed* redshifts were used in the derivation of the distance moduli, so that the derived redshifts are perhaps best characterized as consistency checks, rather than independently estimated values.

5 APPLICATION TO GRB 090423

It is illuminating to apply the above results to prediction of the redshift of GRB 090423, which is thought to have $z \approx 8.2$ (Krimm et al. 2009a, and references therein). The burst was detected by both the Burst Alert Telescope (BAT; Krimm et al. 2009a) and the Fermi Gamma-ray Burst Monitor (GBM; von Kienlin 2009); pertinent information is summarized in Table 2. Additionally, von Kienlin (2009) gives a value of -2.1 ± 0.3 for the exponent β in the Band function (7). The parameter α is 'poorly constrained', and we follow Schaefer (2007) in adopting the representative value $\alpha = -1.1$. It follows that for $1 < z < 8$, the bolometric peak flux $3.1 \times 10^{-7} > P_{\rm bol} > 2.7 \times 10^{-7}$ (BAT) or $2.6 \times 10^{-7} > P_{\rm bol} > 2.3 \times 10^{-7}$ (Fermi GBM).

Spectral lags $\tau_{\rm L}$ were estimated for this burst by Krimm et al. (2009b). Schaefer (2007) recommends that the two spectral channels used should be as widely separated in energy as possible: in this case it implies using the time lag between the 15–25 keV and 50–100 keV bands. The lag is 0.046 (-0.058, $+0.085$) s for the entire burst or 0.021 (-0.032, $+0.054$) for the peak 3 s (figures in brackets are the $\pm 1\sigma$ intervals).

Predictions from the relevant models in Table 1 are given in Table 3. The only models predicting redshifts $z > 3$ are those involving $\tau_{\rm L}$, and better predictions are obtained from the smaller value of $\tau_{\rm L}$. Reducing $\tau_{\rm L}$ to around 0.003 (which is still within the errors) leads to predicted redshifts $\widehat{z} > 8$ – but if accurate determination of such small spectral lags is needed in order to apply Model 2 or 4, these may not be practically useful.

A rough redshift prediction can also be obtained from the Firmani et al. (2006) statistic in (3). Fig. 5 shows the quantity

$$g = \log(10^{6.48}X'') = 6.48 + \log P_{\rm bol} + 0.49 \log T_{0.45} - 0.2 \log(1+z) - 1.62 \log E_{\rm p} \qquad (14)$$

which is plotted on the vertical axis of fig. 7 in Firmani et al. (2006). The data points in Fig. 5 were calculated using data from Schaefer (2007), where available, and $T_{0.45}$ from table 1 in Firmani et al. (2006). The fitted parabola can then be used to estimate redshifts, from calculated values of g.

Table 2. Properties of GRB 090423 and of the BAT and Fermi GBM detectors.

Instrument	$E_{\rm min}$ (keV)	$E_{\rm max}$ (keV)	P (photons s^{-1} cm^{-2})	$E_{\rm p}$ (keV)
BAT	15	350	1.7 ± 0.2	48.6 ± 6.2
Fermi GBM	8	1000	3.3 ± 0.5	54 ± 22

Table 3. Predicted redshifts of GRB 090423, for various models.

Data source	Model 1	Model 2		Model 4	Model 6	
		$\tau_{\rm L} = 0.046$	$\tau_{\rm L} = 0.021$		$\tau_{\rm L} = 0.046$	$\tau_{\rm L} = 0.021$
BAT	2.1	4.7	5.6	2.1	3.6	4.3
Fermi GBM	2.0	4.3	5.2	2.1	3.4	4.1

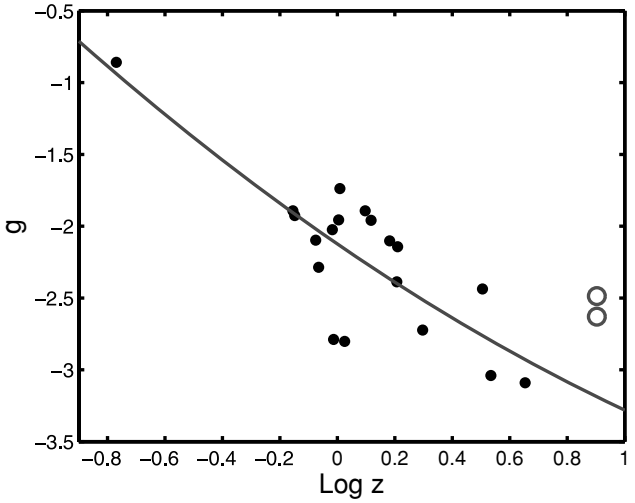

Figure 5. The solid points are calculated values of the Firmani et al. (2006) statistic, in the form given in equation (14). The line is the best-fitting quadratic. The two open circles show approximate values of g for the GRB 090423 data from BAT (top) and Fermi (bottom).

The observable $T_{0.45}$ has not been published, but the 'batgrbproduct Analysis for Trigger = 350184' (http://gcn.gsfc.nasa.gov/notices_s/350184/BA/) gives $T_{0.50} = 5$ s. Replacing $T_{0.45}$ by $T_{0.50}$ in (14) leads to values $g = -2.47$ (BAT) and $g = -2.62$ (Fermi): these are plotted against $z = 8$ in Fig. 5. Predicted redshifts can be read of the curve: these are $\widehat{z} = 1.9$ (BAT) and $\widehat{z} = 2.4$ (Fermi). Since $T_{0.45} < T_{0.50}$ the correct values of g will be slightly lower and the estimated redshifts slightly higher.

6 CONCLUDING REMARKS

(i) Unfortunately the different models in Table 1 cannot be directly compared, as each is based on a different subset of the Schaefer (2007) data. Note though that only two data points used for deriving Model 2 are not included in Model 6, and that the latter has rather smaller scatter, particularly in the predicted redshifts z (compare also Figs 3 and 4). Furthermore, there are clear gains in including other predictors in addition to $P_{\rm bol}$. It therefore seems reasonable to conclude that there are advantages to including multiple predictors.

All models were also fitted to the subset ($N = 28$) of the Schaefer (2007) data for which all variables are available. Models were then compared using the Bayes information criterion (BIC):

$$\mathrm{BIC} = N \log \sigma_e^2 + K \log N \ ,$$

where the first term is a measure of the goodness of the fit (through the residual variance σ_e^2), while the second is a penalty term for the number of parameters K needed to accomplish the fit (e.g. Burnham & Anderson 2004). Since small values of both σ_e^2 and K are in general desirable, the 'best' model is that which minimizes the information criterion. The model containing only $\tau_{\rm L}$ as predictor is optimal according to the BIC; the next best is the model with $\tau_{\rm L}$ and $E_{\rm p}$ as independent variables.

(ii) It appears that little accuracy is lost by using values of $P_{\rm bol}$ calculated with an assumed redshift $z = 1$.

(iii) The dependent variable in the regression models is $y = \log(1 + z)$. It is well known that actual redshifts derived from the inversion

$$z = 10^y - 1 \qquad (15)$$

are biased. It is possible to correct this bias (e.g. Bradu & Mundlak 1970; Duan 1983). Generally these corrections turn out to be very small compared with the prediction errors and are therefore not reported here.

(iv) There has been a debate in the recent literature about the reality of some of the statistical relations which have been found between different GRB observables. In particular, Butler et al. (2007) have argued that some of these may be due to selection effects, rather than being intrinsic to GRBs. In this context, it is important to note that the relations used in Section 3 for prediction were *independent* of the redshift being predicted. The fact that reasonable agreement between observed and predicted redshifts could be obtained suggests real, rather than spurious, relations between redshift and other observables.

(v) It is clear from the material in Section 5 that the predictive power of the various relations is poor for very high redshift GRB. Perhaps the most promising indicator is the spectral lag $\tau_{\rm L}$, but attention will have to be devoted to calculating it as accurately as possible (see also Schaefer 2007). On the other hand, the values of σ_z in Table 1, which were based on prediction of low z, are reasonable. This poses a particular problem for the use of predicted redshifts in statistical studies: the bias properties of the estimators at very high redshifts are unknown, and could lead to unreliable results.

ACKNOWLEDGMENT

Useful suggestions by the referee led to improvements in this paper.

REFERENCES

Atteia J.-L., 2003, A&A, 407, L1
Bradu D., Mundlak Y., 1970, J. Am. Stat. Assoc., 65, 198
Burnham K. P., Anderson D. R., 2004, Sociol. Methods Res., 33, 261
Butler N. R., Kocevski D., Bloom J. S., Curtis J. L., 2007, ApJ, 671, 656
Duan N., 1983, J. Am. Stat. Assoc., 78, 605
Firmani C., Ghisellini G., Avila-Reese V., Ghirlanda G., 2006, MNRAS, 370, 185
Fuller W. A., 1987, Measurement Error Models. John Wiley & Sons, New York
Koen C., 2009, MNRAS, 396, 1499
Krimm H. A., De Pasquale M., Perri M., Stratta G., Ukwatta T. N., 2009a, GCN Rep. 211.1

Krimm H. A., Norris J. P., Ukwatta T. N., Barthelmy S. D., Evans P. A., Gehrels N., Stamatikos M., 2009b, GCN Circ., 9241
Pélangeon A., Atteia J.-L., Lamb D. Q., Ricker G. R., HETE-2 Science Team, 2006, in Holt S. S., Gehrels N., Nousek J.A., eds, AIP Conf. Ser. Vol. 836, Gamma-Ray Bursts in the Swift Era. Am. Inst. Phys., New York, p. 149
Schaefer B. E., 2007, ApJ, 660, 16
von Kienlin A., 2009, GCN Circ., 9229
Yonetoku D., Murakami T., Nakamura T., Yamazaki R., Inoue A. K., Ioka K., 2004, ApJ, 609, 935
Zhang Z.-B., Deng J.-G., Lu R.-J., Gao H.-F., 2006, Chinese J. Astron. Astrophys., 6, 312

This paper has been typeset from a TEX/LATEX file prepared by the author.